Journal of Applied Fluid Mechanics, Vol. 11, No. 1, pp. 1-9, 2018. Available online at www.jafmonline.net, ISSN 1735-3572, EISSN 1735-3645.
DOI: 10.29252/jafm.11.01.28197

Effect of Solvent Contribution on Thermally Developing Flow of FENE-P Fluids between Parallel Plates

A. Filali[1†], L. Khezzar[2], M. Alshehhi[2] and Z. Nemouchi[3]

[1] *Chemical Engineering Department, Imperial College London, London, UK*
[2] *Mechanical Engineering Department, The Petroleum Institute – A part of Khalifa University of Science and Technology, Abu Dhabi, United Arab Emirates*
[3] *LEAP, Mechanical Engineering Department, Université des Frères Mentouri, Constantine, Algeria*

†*Corresponding Author Email: f.abdelkader@ic.ac.uk*

(Received July 10, 2017; accepted October 5, 2017)

ABSTRACT

Numerical computation of thermally developing laminar flow of viscoelastic FENE-P fluids flowing between two stationary parallel plates is investigated using the finite element technique. The influence of the effect of the solvent contribution as well as the fluid rheology on the flow field and heat transfer enhancement is investigated for the case of imposed constant wall heat flux and neglected viscous dissipation. Numerical results for flow field are compared first against available analytical solutions with and without inclusion of the solvent contribution. The obtained results for the viscoelastic case show that increasing Weissenberg number (*We*) leads to an increase in Nusselt number (*Nu*) while high values of the extensibility parameter (L^2) decrease the Nusselt number. Fully developed Nusselt number values for FENE-P fluids flowing between two fixed parallel plates are obtained for several values of polymer concentration and the study confirms quantitatively that polymer concentration enhances heat transfer rates in FENE-P fluids.

Keywords: 2D Thermally developing flow; Rheology; FENE-P model; Solvent contribution; Nusselt number.

NOMENCLATURE

a	parameter related to the fluid physical properties
$\boldsymbol{A}$	conformation tensor
A_c	cross section area
c_p	specific heat
D_h	hydrodynamic diameters
H	half-width of the channel
h_x	local heat transfer coefficient
k	thermal conductivity
L_D	duct length
L^2	extensibility parameter
Nu	average Nusselt number
Nu_x	local Nusselt number
p	pressure
Pr	Prandtl number
p_x	pressure gradient
q_w	heat flux
Re	Reynolds number
T	temperature
U	average velocity
u	velocity
U_N	Newtonian average velocity
We	Weissenberg number
X	dimensionless axial coordinate
x\`	normalized axial coordinate
Y	dimensionless radial coordinate

Greek letters

β	solvent viscosity ratio
λ	relaxation time
θ	dimensionless temperature
η	viscosity
ρ	fluid density
δ	unit tensor
$\boldsymbol{\tau}$	stress tensor

Subscripts

0	vanishing shear rate
b	bulk
i	inlet
p	polymeric
s	solvent
w	wall
x	axial direction
y	radial direction

1. INTRODUCTION

Many industrial applications require the understanding and solution of heat transfer analysis of hydrodynamically fully developed and thermally developing flows. This case that is known as Graetz problem is relevant to different industrial applications, such as heating and cooling processes in ducts of different cross-sections, and the design and optimization of compact heat exchangers in chemical, pharmaceutical and food industries.

Solution of Graetz problem for Newtonian fluids between two parallel plates is well documented by Shah and London (1978). Also, solutions have been obtained for non-Newtonian inelastic fluids of the power law type, see the work of Cotta and Ozisik (1986), Etemad *et al.* (1994) and Jambal *et al.* (2005). The analytical solution of a viscoelastic fluid can only be obtained for fully developed conditions. The drive to understand the flow and heat transfer behaviour of viscoelastic fluids is due to the enhanced heat transfer that can be obtained, see Hartnett and Kostic (1985).

A number of viscoelastic rheological models have been developed over the years exhibiting various degrees of successes in modelling the behavior of real viscoelastic fluids. In contrast to inelastic fluids flowing between parallel plates, relatively fewer investigations were conducted for viscoelastic fluids and were limited to fully developed flow, as indicated in Coelho *et al.* (2003). In addition most of them have used the Phan-Thien-Tanner (PTT) model. Thus, Coelho *et al.* (2003) derived an analytical solution for the simplified version of the PTT model with a linear stress function for two imposed boundary conditions of constant heat flux and constant wall temperature. Previous studies and solutions to the heat transfer problem of the same viscoelastic fluid flowing through pipe and channel geometries were carried out by the same group, Pinho and Oliveira (2000) and Coelho *et al.* (2002) and also by Filali *et al.* (2012). Pinho and Oliveira (2000) investigated the viscous dissipation effect on the heat transfer rate for imposed constant heat flux conditions (q_w = constant), while Coelho *et al.* (2002) investigated similar problem for constant wall temperature condition (T_{wall} = constant). Later, Hashemabadi *et al.* (2004) presented an analytical solution for fully-developed laminar forced convection of SPTT fluids flowing between heated stationary and moving insulated plates. It was reported that viscous heating has a significant effect on decreasing Nusselt number and the influence of the elongational parameter and the Deborah number in increasing the heat transfer coefficient depending on the values of dimensional pressure gradient.

Another model used for polymeric fluids is the non-linear dumbbell model proposed by Peterlin (1966) known as the FENE-P model (Finite Extensible Nonlinear Elastic while P stands for Peterlin). Using such a model, a fully developed solution for the velocity field under laminar conditions was derived by Oliveira (2002) for pipe and channel flows. Later, Oliveira *et al.* (2004) investigated the Graetz problem and developed a semi-analytical solution of a pure FENE-P fluid for tube and slit flow under prescribed constant heat flux and wall temperature. They neglected solvent contribution and took into account the viscous dissipation. Further investigations were carried out numerically by Filali and Khezzar (2013) to study the Graetz problem in ducts using the FENE-P model. Mixing Newtonian solvent with small amount of polymer was reported to show a different behaviour compared to a pure polymeric fluid. That's due to the increased resistance to flow and it was shown by McKinley and Sridhar (2002) and Lindner and Vermant (2003). These dissolved polymers can be found in several industrial applications, such us biopolymer solutions, see Fano (1908) (e.g. plant extracts, bile and egg white), inkjet printing where the polymer concentration and the molecular weight must be chosen carefully for a better printing quality, see Morrison and Harlen (2009) and Hoath *et al.* (2014). In this context, Cruz *et al.* (2005) derived an exact combined solution for the velocity field for fully developed flow in an axisymmetric pipe and plane channel for the affine PTT and FENEP models taking into account a non-zero solvent Newtonian viscosity. It is worth mentioning that no analytical solution can be obtained for three-dimensional geometries as concluded by Khezzar *et al.* (2014) and hence closed form analytical solutions for complex fluid flows, remain confined to a class of problems with simple geometries and fully developed conditions.

While a solution for the hydrodynamic problem of flow between parallel plates using a FENE-P fluid in the fully developed region does exist even with a solvent contribution, it is clear that a solution to the flow and heat transfer problem of developing flow between parallel plates for a FENE-P fluid when the solvent contribution is present does not exist. The present paper aims to fill this gap. The main focus of this paper is the consideration of the effect of the solvent contribution, the fluid viscoelasticity and the rheological parameters of the FENE-P model on heat transfer enhancement for the two dimensional thermally developing entry flows between two stationary parallel plates. In particular, the influence of Weissenberg number (We) and extensibility parameter (L^2) on flow, and specifically the heat rate quantified. The present results of the FENE-P fluids including the effects of the solvent contribution and the fluid rheology on the heat transfer rate can find extensive use in many industrial applications whenever enhanced heat transfer rates are sought.

2. MATHEMATICAL MODEL

The simulation considers a steady laminar flow with constant fluid properties. The FENE-P viscoelastic model is selected in the present study to characterize the Non-Newtonian behaviour of the fluid. The dimensionless governing equations for incompressible non-isothermal viscoelastic flows where obtained by scaling the dimensional equations with the characteristic length (hydraulic diameter (D_h) considered to be equal to 4H for channel flow, were H is the half channel width.), U (average fluid velocity), pressure term with $1/(\rho/U^2)$, the polymeric stress tensor with $D_h/(U(\eta_s+\eta_p))$, where η_s is the zero shear rate solvent viscosity and η_p is the zero shear rate polymeric viscosity. The dimensionless temperature term (θ) is scaled as $\theta = (T-T_i)/(q_w.D_h/k)$, where T_i is the inlet fluid temperature and k is the fluid thermal conductivity. This yields the following dimensionless equations (when viscous dissipation is neglected),

$$\nabla.\boldsymbol{u} = 0 \tag{1}$$

$$(\boldsymbol{u}.\nabla)\boldsymbol{u} = -\nabla p + \frac{\beta}{\mathrm{Re}}\nabla^2\boldsymbol{u} + \frac{1-\beta}{\mathrm{Re}}\frac{1}{We}\nabla.\boldsymbol{\tau}_p \tag{2}$$

$$(\boldsymbol{u}.\nabla)\theta = \frac{1}{\mathrm{Re}\,\mathrm{Pr}}\nabla^2\theta \tag{3}$$

For simplicity, the notation used in Eqs. (1-3) for the unknown variables is similar to the notation used for non-dimensional Navier Stokes equations. In Eq. (2), β, defined as in Eq. (4) represents the ratio of the zero shear rate solvent viscosity to the total zero shear rate viscosity (η)

$$\beta = \eta_s / \eta \tag{4}$$

$$\eta = \eta_s / \eta_p \tag{5}$$

The fluid elasticity is characterized by the Weissenberg number;

$$We = \lambda U / D_h \tag{6}$$

where λ is the relaxation time. The Reynolds number is defined as

$$Re = \rho D_h U / (\eta_s + \eta_p) \tag{7}$$

In Eq. (3), *Pr* is the Prandtl number defined as

$$\mathrm{Pr} = c_p \eta / k \tag{8}$$

The fluid properties are considered to be constant.

In the present study, the polymeric component that is contributing to the stress ($\boldsymbol{\tau_p}$) in Eq. (2) is calculated using the FENE-P viscoelastic model; see Bird *et al.* (1987).

The basis of the FENE-P model has been described in several research papers such us Oliveira (2002), Bird *et al.* (1987), Bird *et al.* (1980) and Purnode and Crochet (1998). The FENE model is used to model long-chained polymers. It represents the polymers by connecting a sequence of beads with nonlinear springs. The FENE model is found to properly model shear-thinning fluids. In Eq. (2), the polymer contribution to the stress needs modelling. Thus, the polymer stress is calculated from:

$$\boldsymbol{\tau}_p = \frac{\eta_p}{\lambda}\left[\frac{\boldsymbol{A}}{1\text{-tr}(\boldsymbol{A})/(L^2)} - a\boldsymbol{\delta}\right] \tag{9}$$

where tr(A) is the trace of the configuration tensor $\boldsymbol{A}$ and $\boldsymbol{A}$ can be obtained from:

$$\frac{\boldsymbol{A}}{1\text{-tr}(\boldsymbol{A})/(L^2)} + \lambda \overset{\nabla}{\boldsymbol{A}} = a\boldsymbol{\delta} \tag{10}$$

where L^2 must always be greater than unity and also appears via the parameter a, which is defined as $a \equiv 1/(1\text{-}3/L^2)$ in Eqs. (9) and (10). Furthermore, when L (or L^2) goes to infinity, the FENE-P model becomes similar to the Maxwell model. The convected derivative by ∇.

In this representation, the temperature dependent factor of $\boldsymbol{A}$ is ignored; see Khezzar *et al.* (2014). This simplification is however, strictly valid only under fully developed conditions. Oliveira (2002) made use of it and with additional simplifications of the momentum equation he was able to obtain his closed form analytical solution. We maintain the same and assume that its influence will remain negligible. While this assumption is introduced in the transport equation for the configuration tensor, the momentum and energy equations remain complete. Local heat transfer coefficient (h_x) is calculated from:

$$q_w = h_x(T_b - T_w), \tag{11}$$

where the fluid bulk temperature denoted by T_b is defined by Shah and London (1978)

$$T_b = \frac{1}{A_c U}\int_{A_c} u.T dA_c \tag{12}$$

Consequently, the local heat transfer coefficient is defined as

$$Nu_x = \frac{h_x H}{k} = \frac{q_w D_h}{k\,(T_w - T_b)} \tag{13}$$

and its average along the pipe length is defined as

$$Nu = \frac{1}{L}\int_0^L Nu_x dx \tag{14}$$

3. NUMERICAL SCHEMES AND METHOD CONVERGENCE

The present simulations are carried out using ANSYS POLYFLOW, the finite element based flow modelling software package. The discrete elastic-viscous split stress (DEVSS) method incorporating the streamline upwinding (SU) scheme is used to improve convergence and deal with the numerical instabilities related to the non-linear terms in the modelling of viscoelastic flows. Additional to the DEVSS/SU technique, the use of an evolution variable to deal with the viscoelastic stress terms was necessary. The technique can be applied directly to the parameters that cause non-linearity such as the relaxation time (λ). In this case, the relaxation time value is reduced to a minimum value allowing a successful convergence of the problem, then it is increased gradually by an incremental step until the final set value is reached. Convergence of the numerical computation in POLYFLOW is ensured when the relative error for each variable (p, u and τ) reaches 10^{-4}.

4. GEOMETRY, BOUNDARY CONDITIONS AND MODEL MESHING

The present work addresses itself to the determination of Nusselt number and the hydrodynamic behaviour of FENE-P fluid flowing in a 2D channel duct. The imposed boundary conditions can be summarized as follows:

- At the inlet section, X = 0, a fully developed velocity profile and constant temperature ($\theta = 0$) are imposed.
- At the wall, Y = y/D_h, no-slip condition u = v = 0 and a uniform heat flux q_w are applied.
- At the symmetry axis, Y = 0, $\partial\theta/\partial Y = 0$.
- At the outlet, X=L_D/D_h, outflow boundary conditions are applied.

Figure 1 illustrates the geometry and boundary conditions considered in the present simulation.

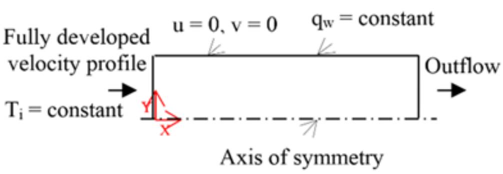

Fig. 1. Geometry for flow between parallel plates and boundary conditions.

The local Nusselt number variations are presented and plotted versus the normalized longitudinal distance (x`) where $x$` = *x/H.Re.Pr*. The assumed value of the Prandtl number *Pr* = 30.

A grid sensitivity study was conducted considering the variation of the Nusselt number for *We* = 10 and L^2 = 10 to obtain optimum mesh size that can be used to obtain accurate results with a minimum computational cost. Results for the three different meshes used are shown in Fig. 2. A minor difference is exhibited between meshes M2 and M3. Hence, to optimize the numerical calculations, mesh M2 is considered in all computations of the present study.

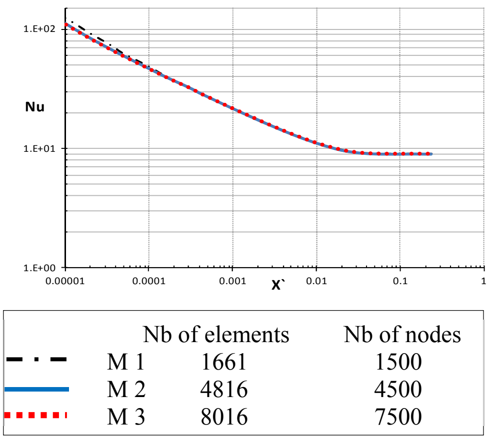

Fig. 2. Mesh independency test for 2D channel case: heat transfer coefficient vs. normalized longitudinal distance x` for *We* = 10, L^2 = 10.

5. RESULTS AND DISCUSSION

The results presented in this analysis are reported for FENE-P viscoelastic fluids flowing between fixed parallel plates under constant heat flux boundary condition. The main aim here is to seek to quantify the effect of the solvent concentration (β) which can take values in the interval [0, 1] on flow parameters such as the axial velocity, stress profiles, but mainly on the Nusselt number with L^2 and *We* as parameters. A zero value of β corresponds to zero solvent viscosity and 1 to a purely viscous Newtonian fluid. The numerical results for the velocity and stress profiles are compared with the existing analytical solution developed by Cruz *et al.* (2005), for a pure polymeric FENEP fluid in which the solvent viscosity ratio is very small $\beta \approx 0$, which correspond also with the analytical solution developed by Oliveira (2002) for $\beta = 0$. Only Sample results for $\beta = 0$ will be presented here for validation and comparison purposes. Extensive results for pure polymeric FENE-P fluid can be found in a previously published paper, see Filali *et al.* (2014), in which important results showing the effect of *We* and L^2 on the Nusselt number were presented for two imposed boundary conditions; constant heat flux (q_w=constant) and constant wall temperature (T_{wall}=constant).

Subsequently, the solvent contribution effect is considered ($\beta \neq 0$) for an imposed constant heat flux thermal boundary condition and the analytic solution for velocity distribution of Cruz *et al.* (2005), is used as a benchmark and validation for the present approach. The results of the FENE-P fluid flowing within a plane-parallel duct will then contribute and provide extensive numerical results to the heat transfer problem. This is done by examining the effect of β on the calculated Nusselt number in the thermally developing region for high level of elasticity and extensibility parameter as well as the effect of β on the fully developed Nusselt number for different values of the parameter $We^2/(aL)^2$.

5.1 Results Without Solvent Contribution ($\beta = 0$)

For a pure polymeric FENE-P fluid $\beta = 0$, Cruz *et al.* (2005) obtained a theoretical solution for the velocity profile of fully developed flow between parallel plates for a FENE-P fluid with solvent contribution. This solution is used to benchmark the numerical solution obtained herein:

$$u(y) = \left(\frac{6U_N}{\beta}\right)\left(1-\left(\frac{y}{H}\right)^2\right) + \frac{3}{8C\eta_s}\left\{F_R^+G_R^- - F_r^+G_r^- + F_R^-G_R^+ - F_r^-G_r^+\right\} \quad (15)$$

where

$$U_N = \frac{-p_x H^2}{12\eta_0} \quad (16)$$

where η_0 is the shear-thinning viscosity for vanishing shear rate and the functions F and G are defined as:

$$F_X^{\pm} = \left(CX \pm \sqrt{M^3 + (CX)^2} \right)^{\frac{1}{3}}$$
$$G_X^{\pm} = 3CX \pm \sqrt{M^3 + (CX)^2} \tag{17}$$

and

$$M = \frac{\eta_p^2 (b+5)^3}{6\lambda^2 (b+2)^2} \left(1 + \frac{\eta_p}{\eta_s} \right); \tag{18}$$

$$N = \left(\frac{\eta_p^2 (b+5)^3}{4\lambda^2 (b+2)^2} \frac{\eta_p}{\eta_s} p_x \right) y = Cy$$

The comparisons of the velocity profiles against the existing theoretical solution of Cruz *et al*. (2005) are shown in Fig. 3 and 4.

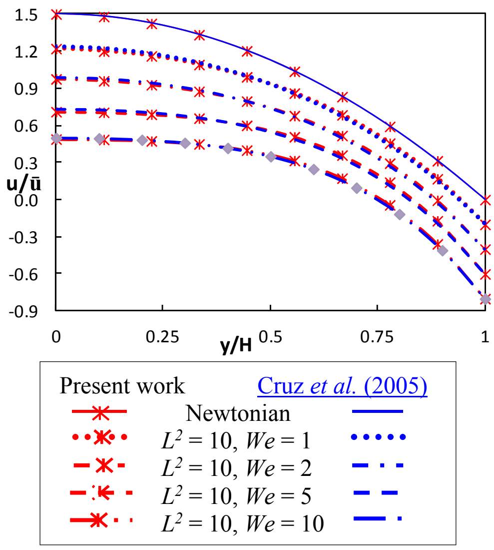

Fig. 3. Predicted velocity profiles for $\beta = 0$, L^2=10 and varying *We*.

Excellent agreement can be observed between the present numerical profiles and the analytical profiles of Cruz *et al*. (2005) for the FENE-P and Newtonian fluids. It was reported in the analysis of the effect of *We* and L^2 on the flow that these two parameters have an opposite effect on the velocity profiles which tends to be flatter for low extensibility values and high elasticity levels due to the enhanced shear-thinning behaviour, see Filali *et al*. (2014). The same effect of *We* and L^2 was reported for the heat transfer results where increasing *We* to a value of 10 for constant value of L^2 =10, increases Nusselt number by 9% and 10.1% over the Newtonian value for both imposed boundary conditions (q_w = constant, T_w = constant). On the other hand increasing L^2 from 10 to 1000 decreases the heat transfer coefficient. The physics behind the enhanced heat rate for viscoelastic fluids characterized by the shear-thinning behaviour can be explained by the changes in the flow field as a result of the reduced fluid viscosity. This change affects the temperature field by increasing the fluid bulk temperature and as a consequence decreases the temperature difference (T_w-T_b) used in the determination of heat transfer rate.

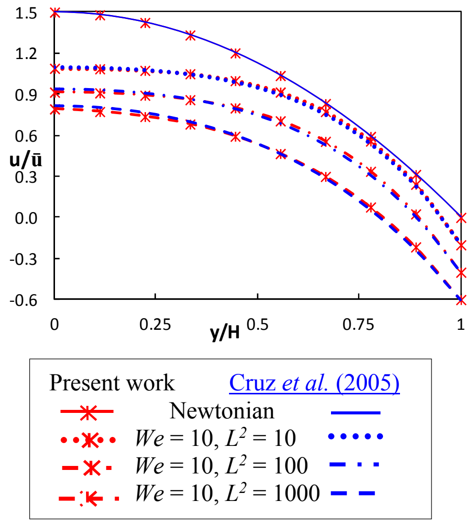

Fig. 4. Predicted velocity profiles for $\beta = 0$, *We*=10 and varying L^2.

5.2 Results With Solvent Contribution (β≠0)

Next, results including the effect of the solvent contribution (meaning when β ≠ 0) are presented. Figure 5a shows fully developed velocity profiles for β = 0.3, L^2=10 while varying *We*. The numerical solution is shown to agree perfectly with the theoretical velocity profile given by Eq. (15). The small difference in the core velocity remains way below 1%. The effect of *We* can also be clearly seen in Fig. 5b in good agreement with the theoretical solution, i.e. an increase in *We* leads to a small decrease in the core velocity. The same trend was predicted for the axisymmetric geometry by Khezzar *et al*. (2014) but the influence of *We* on the core velocity in that case was much more pronounced.

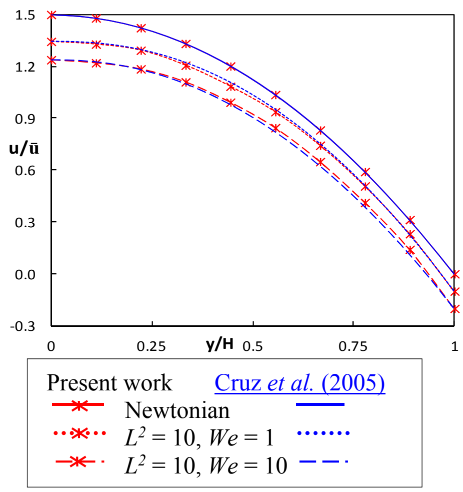

Fig. 5a. Predicted fully developed velocity profiles against analytic solution of Cruz *et al*. (2005) for $\beta = 0.3$, $L^2 = 10$ and varying *We* (*We* = 1 and 10).

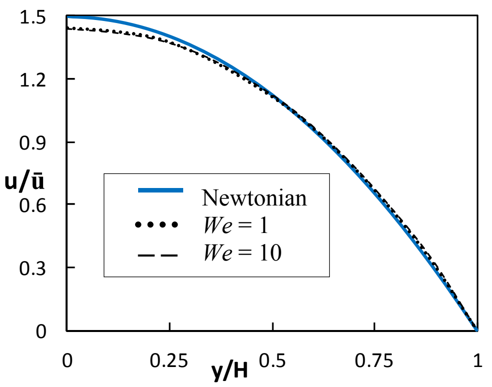

Fig. 5b. Velocity profiles for constant L^2 = 10 and β = 0.3 and varying *We*.

For a constant value of the polymer concentration β = 0.3, and a constant value of *We* = 10, the influence of the extensibility parameter L^2 on the velocity profile is depicted on Fig. 6a. A good agreement between the present numerical predictions and the theoretical solution of Cruz *et al.* (2005) is shown in Fig. 6a with a difference less than 1%. Furthermore, the trend of the effect of increasing L^2 leading to a flatter velocity profile is predicted correctly, see Fig. 6b.

The polymeric shear stress component could be obtained explicitly by solving Eq. (19); see Cruz *et al.* (2005)

$$\frac{du(y)}{dy}=\frac{p_x y}{\eta_s}-\frac{1}{\eta_s}\tau_{yx} \qquad (19)$$

where

$$\tau_{yx}=\left(\sqrt[3]{Cy+\sqrt{A^3+(Cy)^2}}+\sqrt[3]{Cy-\sqrt{A^3+(Cy)^2}}\right) \qquad (20)$$

and M and C are constant factors defined by Eq. (18). The axial normal stress is given by Eq. (21).

$$\tau_{xx}=\frac{2\lambda}{\eta_p}\tau_{yx}^2 \qquad (21)$$

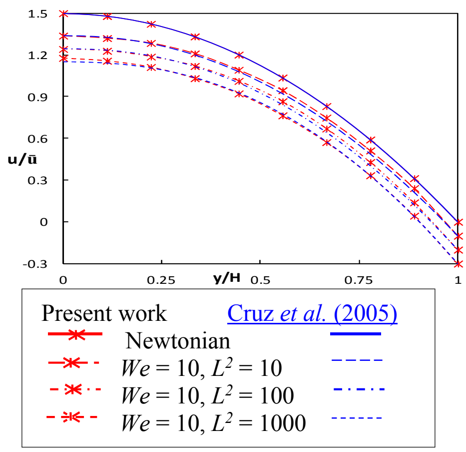

Fig. 6a. Predicted fully developed velocity profiles against analytic solution of [Cruz *et al.* (2005)] for *β* = 0.3, *We* = 10 and varying L^2 (L^2 = 10, 100 and 1000).

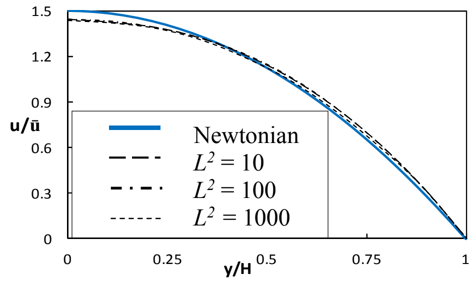

Fig. 6b. Velocity profiles for constant *We* = 10 and β = 0.3 and varying L^2 (L^2 = 10, 100 and 1000).

Figures 7a and b show the profiles of the normalized total extra stress for the axial and tangential components respectively. A very good agreement is shown between the numerical and the theoretical solution of Cruz *et al.* (2005) given by Eq. (15).

In Fig. 7a, the normal stress component shows a marked decrease when β increases to reach 1 as the polymer concentration decreases. In such conditions the behaviour approaches that of a Newtonian fluid. As for the shear stress component plotted in Fig. 7b, increasing the polymer concentration when β is decreased, leads to a decrease in the shear stress levels to lower values due to the shear thinning behaviour which becomes more important.

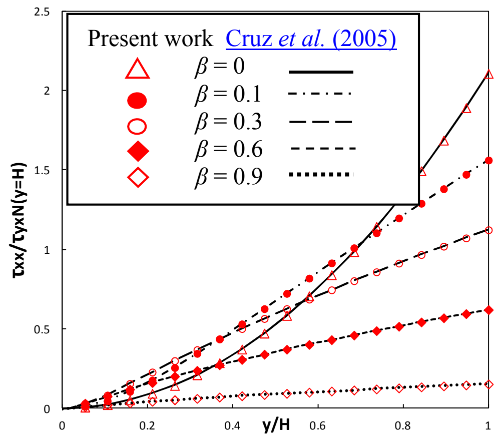

Fig. 7a. Normalized normal stress profiles for fixed *We* = 10, L^2 = 10 and varying β.

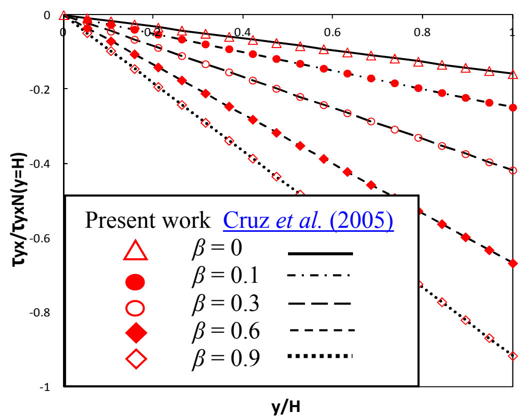

Fig. 7b. Normalized shear stress profiles for fixed *We* = 10, L^2 = 10 and varying β.

Figure 8 represents the effect of the polymer concentration on the dimensionless temperature profile for a constant fluid elasticity and extensibility parameter (We = 10 and L^2 = 10). Results indicate that increasing the fluid concentration leads to an increase in the temperature profile specifically near the wall region which will degrade the heat transfer rate.

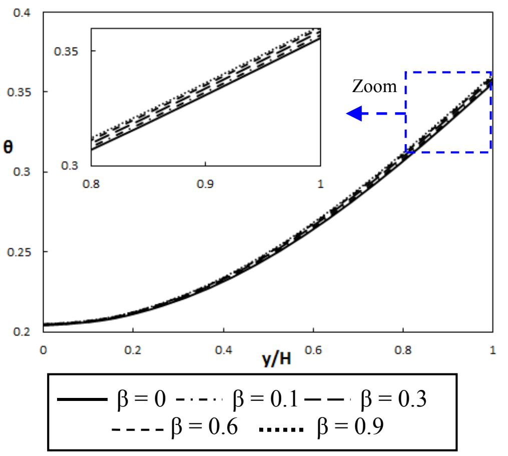

Fig. 8. Normalized temperature profiles for fixed *We* = 10, L^2 = 10 and varying β.

Figure 9, shows that combination of increasing We or decreasing L^2 defined by the ratio $We^2/(aL)^2$ (for $We^2/(aL)^2 < 20$) leads to a decrease in the temperature profile specially near the wall region. This is due to the intensified shear-thinning effects that affect the velocity profiles which become flatter and leading to a higher shear rate near the wall and therefore improving the heat transfer rate. For $We^2/(aL)^2 > 20$, no changes are observed in the temperature profiles and therefore, Nusselt number becomes constant and reaches an asymptotic value. This is clearly shown later in Fig. 11.

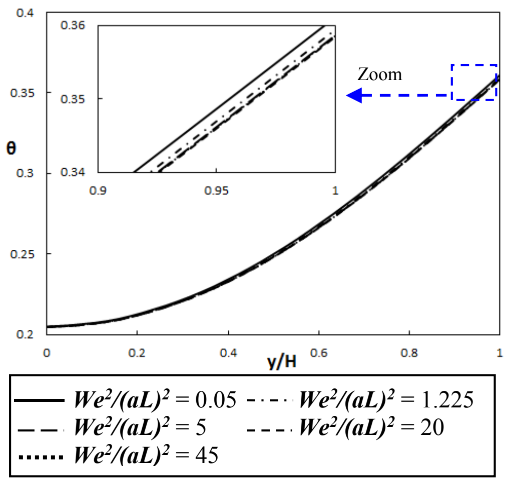

Fig. 9. Normalized temperature profiles for fixed β = 0.3 and varying ratio $We^2/(aL)^2$.

For many entry flow problems in industry, the thermal entry length is an important parameter that needs to be characterized since it can affect the performance of an industrial device. Therefore, it is important to analyse the heat transfer rate in both, the developing and fully developed regions.

Figure 10 represents the effect of the polymer concentration (β) on the calculated local Nusselt number in both, the thermally developing and fully developed regions at high levels of elasticity and extensibility parameter (We = 10 and L^2 = 10). Results indicate that the highest values of the Nusselt number can be obtained for the case of pure polymeric fluid (β = 0) while increasing the solvent concentration ($\beta \to 1$) provides a heat transfer coefficient closer to the Newtonian limit. Results also show that the polymer concentration and the fluid rheology do not affect the thermal entry length which is found to be similar for both Newtonian and viscoelastic fluids. This confirms that similar to Newtonian fluids, the thermal entry length for viscoelastic fluids, depends only on Re and Pr number.

To cover the combined effect of the different parameters such as β, We and L^2, on the heat transfer enhancement, results in Fig. 11 represent the variation of the fully developed Nusselt number versus the ratio $We^2/(aL)^2$ with the polymer concentration taken as a parameter for the case of a prescribed constant wall heat flux. Increasing $We^2/(aL)^2$ leads to a monotonic increase in the Nusselt number from the well-known Newtonian value of 8.235 to reach an asymptotic limit of 9.08754 for the lowest solvent concentration or pure polymer case (β = 0) where shear thinning behaviour is more pronounced. This represents a net increase of 10.35%. It is interesting to note that for a fixed value of β the Nusselt number increases rapidly to its asymptotic value.

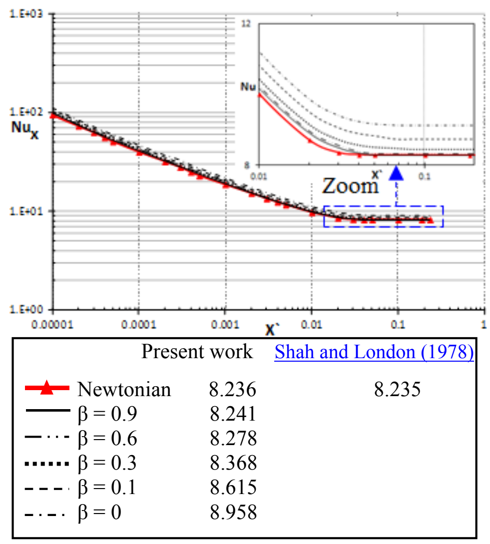

Fig. 10. Effect of solvent contribution *β* on the variation Nusselt number versus normalized longitudinal distance *x`*, for *We* = 10 and L^2 = 10.

This is usually achieved for a value of $We^2/(aL)^2$ of about 20 and sometimes lower for larger β values. This means that large values of $We^2/(aL)^2$ have no influence on the Nu . A similar behaviour was predicted by Oliveira *et al.* (2004) and Khezzar *et al.*

(2014) for the case of the axisymmetric geometry and is typical of FENE-P fluids. It is worth mentioning also that for ($\beta > 0.5$), there is no significant enhancement of the fully developed Nusselt number which tends towards a value close to the Newtonian limit.

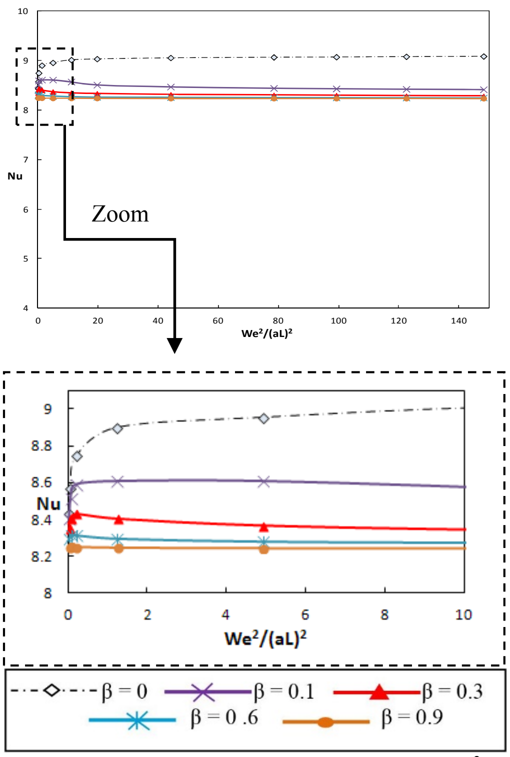

Fig. 11. Nusselt number vs. the parameter $We^2/(aL)^2$, under imposed heat flux, positive q_w, effects of the viscosity ratio β.

6. CONCLUSION

Heat transfer and flow behavior of FENE-P fluid flowing between two stationary plates is investigated numerically using the POLYFLOW commercial code. The effect of the solvent concentration on this flow and heat transfer was assessed for an imposed constant heat flux condition. The study investigated the effects of the rheological parameters such as Weissenberg number (*We*) which defines the fluid elasticity, the extensibility parameter (L^2) and the polymeric concentration through the parameter β on the flow field and Nusselt number.

The results of the flow simulations have shown an excellent agreement between the theoretical and numerical velocity fields. This serves to validate both the numerical approach and provide further confirmation of the theoretical results.

For the FENE-P fluid, it was shown that increasing the elasticity (through Weissenberg number (*We*)) or decreasing the extensibility parameter (L^2) enhances the Nusselt number due to the enhanced shear-thinning behavior of FENE fluids. The increase can reach up to 10% over the Newtonian value. It was also found that for a constant polymer concentration the effect of the parameter $We^2/(aL)^2$ on enhancing the heat rate vanishes rapidly beyond values just above 20. The present results of the heat transfer for FENE-P fluids flowing between parallel plates with different solvent concentrations will contribute and provide useful knowledge of the development and the design of industrial applications using plane passages where heat transfer enhancement is sought.

REFERENCES

Bird, R. B., C. F. Curtiss, R. C. Armstrong and O. Hassager (1987). *Dynamics of Polymeric Liquids Kinetic Theory* 2, second ed., Wiley, New York.

Bird, R. B. Dotson, P. J. and N. L. Johnson (1980). Polymer solution rheology based on a finitely extensible bead-spring chain model, *J. Non-Newt. Fluid Mech* 7, 213-235.

Coelho, P. M., F. T. Pinho and P J. Oliveira (2003). Thermal entry flow for a viscoelastic fluid: the Graetz problem for the PTT model. *Int. J. Heat and Mass Transfer* 46, 3865-3880.

Coelho, P. M., F. T. Pinho and P. J. Oliveira (2002). Fully developed forced convection of the Phan-Thien–Tanner fluid in ducts with a constant wall temperature, *Int. J. Heat Mass Transfer* 45, 1413–1423.

Cotta, R. M. and M. N. Ozisik, (1986). Laminar forced convection to non-Newtonian fluids in ducts with prescribed wall heat flux, *Int Commun Heat Mass Transfer* 13, 325–334.

Cruz, D. O. A., F. T. Pinho and P. J. Oliveira (2005). Analytical solutions for fully developed flow of some viscoelastic liquids with a Newtonian solvent contribution. *J. Non-Newt. Fluid Mech* 132, 28-35.

Etemad, S. G., A. S. Mujumdar and B. Huang (1994). Viscous dissipation effects in entrance region heat transfer for a power law fluid flowing between parallel plates, *Int. J. Heat Fluid Flow* 15, 122–131.

Fano, G. (1908). Contributo allo studio dei corpi filanti, Archivio di fisiologia (Contribution to the study of thread-forming materials. Physiology Archive) 5, 365–370.

Filali, A., L. Khezzar and Z. Nemouchi (2014). Entry flows for FENE-P fluids in a plane passage for constant heat flux & wall temperature boundary conditions. Proceedings of CONV-14: Int. Symp. on Convective Heat and Mass Transfer 8 – 13.

Filali, A. and L. Khezzar (2013). Numerical Simulation of the Graetz Problem in Ducts with Viscoelastic FENE-P Fluids" Computers and Fluids 84, 1-15.

Filali, A., Khezzar, L., Nemouchi, Z., Siginer, D.A. (2012). Graetz Problem with Non-linear Viscoelastic Fluids in Non-Circular Tubes. *International Journal of Thermal Sciences* 61, 50-60.

Hartnett, J. P. and M. Kostic (1985). Heat transfer to a viscoelastic fluid in laminar flow through a rectangular channel. *Int. J. Heat Mass Transfer* 28, 1147-1155.

Hashemabadi, S. H., S. G. Etemad and J. Thibault (2004). Forced-convection heat transfer of Couette-Poiseuille flow of non-linear viscoelastic fluids between parallel plates, *Int. J. Heat Mass Transfe* 47, 3985–3991.

Hoath, S. D., D. C. Vadillo, O. G. Harlen, C. McIlroy, N. F. Morrison, W. K. Hsiao, T. R. Tuladhar, S. Jung, G. D. Martin and I. M. Hutchings (2014). Inkjet printing of weakly elastic polymer solutions, *J. Non-Newt. Fluid Mech.* 205, 1–10 .

Jambal, O. T. Shigechi, G. Davaa and S. Momoki (2005). Effects of viscous dissipation and fluid axial heat conduction on heat transfer for non-Newtonian fluids in ducts with uniform wall temperature. Part I: Parallel plates and circular ducts, *Int. Commun. Heat Mass Transfer* 32, 1165–1173.

Khezzar, L., A. Filali and M. AlShehhi (2014). Flow and Heat Transfer of FENE-P Fluids in Ducts of Various Shapes: Effect of Newtonian Solvent Contribution *J. Non-Newt. Fluid Mech.* 207, 7-20.

Lindner, A., J. Vermant and D. Bonn (2003). How to obtain the elongational viscosity of dilute polymer solutions *Physica A* 319, 125–133.

McKinley, G. H. and T. Sridhar (2002). Filament-stretching rheometry of complex fluids, *Ann. Rev. Fluid Mech* 34, 375–405.

Morrison, N. F. and O. G. Harlen (2009). Viscoelasticity in inkjet printing, *Rheol. Acta.* 49, 619–632.

Oliveira, P. J., P. M. Coelho and F. T. Pinho (2004). The Graetz problem with viscous dissipation for FENE-P fluids. *J. Non-Newt. Fluid Mech* 121, 69–72.

Oliviera, P. J. (2002). An exact solution for tube and slit flow of a FENE-P fluid, *Acta Mechanica* 158, 157-167.

Peterlin, A. (1966). Hydrodynamics of macromolecules in a velocity field with longitudinal gradient. *Journal of Polymer Science Part B: Polymer Letters* 4, 287–291.

Pinho, F. T. and P. J. Oliveira (2000). Analysis of forced convection in pipes and channels with the simplified Phan-Thien–Tanner fluid, *Int. J. Heat Mass Transfer* 43, 2273–2287.

Purnode, B. and M. J. Crochet (1998). Polymer solution characterization with the FENE-P model, *J. Non-Newt. Fluid Mech* 77, 1-20.

Shah, R. K. and A. L. London (1978). *Laminar flow forced convection in ducts*, Academic Press, New York.